Nanoscale and Microscale Thermophysical Engineering, 11: 121–128, 2007

ISSN: 1556-7265 print / 1556-7273 online
DOI: 10.1080/15567260701337423

A HARD CONSTRAINT ALGORITHM TO MODEL PARTICLE INTERACTIONS IN DNA-LADEN FLOWS

D. Trebotich
Center for Applied Scientific Computing, Lawrence Livermore National Laboratory, Livermore, California, USA

G.H. Miller
Department of Applied Science, University of California, Davis, California, USA

M.D. Bybee
Department of Chemical and Biomolecular Engineering, University of Illinois at Urbana—Champaign, Urbana, Illinois, USA

We present a new numerical method for particle interactions in polymer-fluid models of DNA-laden flows. The DNA is represented by a bead-rod polymer model and is fully-coupled to the fluid. The main objective in this work is to properly model polymer-polymer and polymer-surface interactions by enforcing the physical rod-rod and rod-surface non-crossing constraints. Our new method is based on a rigid constraint algorithm whereby rods elastically bounce off one another to prevent crossing, similar to our previous algorithm used to model polymer-surface interactions.

KEY WORDS: microfluidics, fluid-polymer coupling, viscoelasticity, Navier-Stokes, multiscale computational modeling

INTRODUCTION

Microfluidic devices are increasingly important in biodefense and biomedical applications including pathogen detection, continuous monitoring, and drug delivery. Numerical algorithms that can model flows of complex biological fluids within these devices are needed for further development and optimization. Biological fluids, *in vivo* and *in vitro* can be well-approximated as an aqueous solvent with numerous high molecular weight polymeric solutes. In biological flows, as in microfluidic devices, the suspended polymers interact with one another and interact with the confining surfaces. A numerical polymer-fluid model must respect the same physical constraints as the actual system in order for the computed flows to have predictive value. The

This work was performed under the auspices of the U.S. Department of Energy by the University of California, Lawrence Livermore National Laboratory under contract No. W-7405-Eng-48. The work of G.H. Miller at the University of California, Davis, was supported by LLNL IUT subcontract number B550201 and partially supported by DOE MICS contract number DE-FG02-03ER25579. The work of M.D. Bybee at the Lawrence Livermore National Laboratory was supported by the Department of Energy Computational Science Graduate Fellowship Program under grant number DE-FG02-97ER25308.

Address correspondence to D. Trebotich, Lawrence Livermore National Laboratory, P.O. Box 808, L-560 Livermore, CA 94551. E-mail: trebotich1@llnl.gov

problem is complicated due to the time scale of the associated short-range interactions being much smaller than the time scales of the bulk fluid, necessitating multiscale schemes.

In previous work we developed a model that coupled bead-rod polymers to an incompressible viscous solvent [1]. We took care to conservatively couple the polymer and solvent forces — both viscous and stochastic — in order that the fluid "feel" the effect of the polymer. It is in this sense of obeying Newton's third law of motion that we consider the dynamics to be "tightly coupled". (The purpose of the full-coupling is to be able to simulate the effects of a large number of polymers and to compare this hybrid approach with a viscoelastic continuum model as in Trebotich et al. [2].) Additionally, the polymer nodes may experience elastic collisions with domain boundaries, thereby enforcing the physical constraint that the polymers remain confined to the fluid. With this numerical algorithm, we have been able to simulate polymer-boundary interactions which occur in DNA size-separation and extraction devices. We have also obtained preliminary results for more complicated 2D and 3D device geometries [3]. Our model captures many essential features observed in DNA visualization experiments [4]. In particular, the molecule tends to extend in regions of large shear flow, and contract in its absence.

However, to model the probable fate of individual molecules in microfluidic systems or biological flows, it is desirable to incorporate more physically-realistic behavior. For polymer models of DNA, of immediate concern is the non-crossing constraint: a polymer section cannot pass through another polymer section. In our previous freely-jointed bead-rod model, as with many other current implementations (e.g., Somasi et al. [5]), crossing of rod sections is allowed. We treated polymer-surface interactions as purely elastic collisions, and we do not treat polymer-polymer interactions at all. The resulting behavior has a strong theoretical foundation (e.g., Mazars [6]) and is therefore important for algorithm validation, but does not respect the correct non-crossing physical behavior of real molecules.

Furthermore, macromolecules like DNA are charged and chemically active. They interact through screened Coulombic interactions and migrate in response to imposed electric fields. In addition, microfluidic separators have been designed based on the increase of residence time with molecule length in packed bed and pillared array geometries, or through chemically mediated residence time enhancement achieved by binding selective proteins to channel surfaces. These physical effects are characterized by intra-polymer, inter-polymer, and polymer–surface interaction potentials that may be long-ranged.

In this paper we will explore the rod-crossing problem using rigid constraints. An alternative approach is to use short-range or "soft" potentials, to achieve the same ends. We have explored those methods also, but the focus of this paper is the implementation of "hard" constraints. A preliminary version of this work can be found in Bybee et al. [7].

ALGORITHMIC APPROACH

We present here a new hard constraint algorithm, which enforces the non-crossing constraint by elastically bouncing the polymer when it comes in contact with itself. This approach to rod-rod non-crossing is similar to that used to prevent polymer-surface crossing in microfluidic post array channels [1].

Rod–Rod Uncrossability Constraint

The rod–rod uncrossability constraint works by detecting rod–rod collisions and treating them as elastic collisions between infinitely thin rods. It is similar to the bead–surface uncrossability constraint already implemented in Trebotich et al. [1]. For simplicity of exposition the algorithm in 3D is outlined below as an extension to the existing algorithm in [1]. Steps 1, 2, and 4 are described in more detail in [1]. The ideas for steps 3a-3d have been taken from [9]. In that work bonds are considered as elastic bands between bonded particles. When any two of these elastic bands make contact, an entanglement point is created which prevents them from crossing. We call this a hard constraint algorithm as it is an end member of a classical smooth potential that requires no parameter tuning.

The polymer is represented by a series of beads connected by rigid rods. The bead positions and velocities are given by x and v respectively. Rod i is defined as the line segment from bead i to bead $i+1$, or from x_i to x_{i+1}.

For each time step, beginning with $\boldsymbol{x}^n$ and $\boldsymbol{v}^n$:

1. Calculate the unconstrained motion to obtain $\boldsymbol{x}^*$ and $\boldsymbol{v}^*$.
2. Calculate the motion subject to the rod length constraint to obtain $\boldsymbol{x}^\dagger$ and $\boldsymbol{v}^\dagger$.
3. Calculate the motion subject to the rod-rod uncrossability constraint to obtain $\boldsymbol{x}^\ddagger$ and $\boldsymbol{v}^\ddagger$. The details of this step are as follows:

   Calculate $\boldsymbol{v}^{\Delta t}$, the bead velocities over the current time step

$$\boldsymbol{v}^{\Delta t} = (\boldsymbol{x}^\dagger - \boldsymbol{x}^n)/\Delta t$$

   so that the time-linear trajectory of each bead over the current time step is

$$\boldsymbol{x} = \boldsymbol{x}^n + \boldsymbol{v}^{\Delta t} t \quad t \in (0, \Delta t) \tag{1}$$

   Repeatedly loop through all rod pairs until no more collisions are detected. For each pair of rods i and j:

   3a. Calculate the triple product V_{ij} at times 0 and Δt where

$$V_{ij} = (\boldsymbol{x}_i - \boldsymbol{x}_j) \cdot ((\boldsymbol{x}_{i+1} - \boldsymbol{x}_i) \times (\boldsymbol{x}_{j+1} - \mathbf{x}_j)) \tag{2}$$

   The value of V_{ij} will be zero if the infinite lines containing the rods intersect or are parallel. Therefore, if the value of V_{ij} changes sign over the time step, a possible rod-rod crossing has occurred. Otherwise, proceed to step 3k.

   3b. Calculate τ, the time of crossing. Substituting the time-linear trajectories of (1) into (2) gives a third-order polynomial in t for V_{ij}. The smallest root of this polynomial in the range $(0,\Delta t)$ will be τ.

   To simplify the calculation, let

$$\alpha = \boldsymbol{x}_i - \boldsymbol{x}_j = \alpha_0 + \alpha_1 t$$
$$\beta = \boldsymbol{x}_{i+1} - \boldsymbol{x}_i = \beta_0 + \beta_1 t$$
$$\gamma = \boldsymbol{x}_{j+1} - \boldsymbol{x}_j = \gamma_0 + \gamma_1 t$$

where

$$\alpha_0 = \boldsymbol{x}_i^n - \boldsymbol{x}_j^n$$
$$\alpha_1 = \boldsymbol{v}_i^{\Delta t} - \boldsymbol{v}_j^{\Delta t}$$
$$\beta_0 = \boldsymbol{x}_{i+1}^n - \boldsymbol{x}_i^n$$
$$\beta_1 = \boldsymbol{v}_{i+1}^{\Delta t} - \boldsymbol{v}_i^{\Delta t}$$
$$\gamma_0 = \boldsymbol{x}_{j+1}^n - \boldsymbol{x}_j^n$$
$$\gamma_1 = \boldsymbol{v}_{j+1}^{\Delta t} - \boldsymbol{v}_j^{\Delta t}$$

The coefficients of the polynomial $V_{ij} = a_3 t^3 + a_2 t^2 + a_1 t + a_0$ are then given by

$$a_0 = \alpha_0 \cdot (\beta_0 \times \gamma_0)$$
$$a_1 = \alpha_0 \cdot (\beta_1 \times \gamma_0) + \alpha_1 \cdot (\beta_0 \times \gamma_0) + \alpha_0 \cdot (\beta_0 \times \gamma_1)$$
$$a_2 = \alpha_1 \cdot (\beta_1 \times \gamma_0) + \alpha_0 \cdot (\beta_1 \times \gamma_1) + \alpha_1 \cdot (\beta_0 \times \gamma_1)$$
$$a_3 = \alpha_1 \cdot (\beta_1 \times \gamma_1)$$

3c. Calculate $\boldsymbol{x}^\tau$, the bead positions at time τ.

$$\boldsymbol{x}^\tau = \boldsymbol{x}^n + \boldsymbol{v}^{\Delta t}\tau$$

3d. Calculate χ, the point of intersection at time τ, by solving the following set of equations:

$$\chi = \boldsymbol{x}_i^\tau + \lambda_i\left(\boldsymbol{x}_{i+1}^\tau - \boldsymbol{x}_i^\tau\right) = \boldsymbol{x}_j^\tau + \lambda_j\left(\boldsymbol{x}_{j+1}^\tau - \boldsymbol{x}_j^\tau\right)$$

where λ_i and λ_j define the point of intersection between the lines containing rods i and j respectively. If $(0 \le \lambda_i \le 1)$ and $(0 \le \lambda_j \le 1)$ then the point of intersection lies on both rods and a rod-rod crossing has occurred. Otherwise, proceed to step 3k.

3e. Calculate $\boldsymbol{n}$, the unit vector normal to the plane formed by the two rods at time τ

$$\boldsymbol{n} = \frac{\left(\boldsymbol{x}_{i+1}^\tau - \boldsymbol{x}_i^\tau\right) \times \left(\boldsymbol{x}_{j+1}^\tau - \boldsymbol{x}_j^\tau\right)}{\left|\left(\boldsymbol{x}_{i+1}^\tau - \boldsymbol{x}_i^\tau\right) \times \left(\boldsymbol{x}_{j+1}^\tau - \boldsymbol{x}_j^\tau\right)\right|}$$

3f. Calculate $\boldsymbol{v}_{\text{rel}}^{\Delta t}$, the relative velocity of the intersection point over the current time step

$$\boldsymbol{v}_{\text{rel}}^{\Delta t} = \left(\boldsymbol{v}_j^{\Delta t} - \boldsymbol{v}_i^{\Delta t}\right) + \lambda_j\left(\boldsymbol{v}_{j+1}^{\Delta t} - \boldsymbol{v}_j^{\Delta t}\right) - \lambda_i\left(\boldsymbol{v}_{i+1}^{\Delta t} - \boldsymbol{v}_i^{\Delta t}\right)$$

3g. Calculate $\boldsymbol{v}^{\text{col}}$, bead velocities after collision

$$\boldsymbol{v}_i^{\text{col}} = \boldsymbol{v}_i^{\Delta t} + 2(1 - \lambda_i)\left(\boldsymbol{n} \cdot \boldsymbol{v}_{\text{rel}}^{\Delta t}\right)\boldsymbol{n}$$
$$\boldsymbol{v}_{i+1}^{\text{col}} = \boldsymbol{v}_{i+1}^{\Delta t} + 2\lambda_i\left(\boldsymbol{n} \cdot \boldsymbol{v}_{\text{rel}}^{\Delta t}\right)\boldsymbol{n}$$
$$\boldsymbol{v}_j^{\text{col}} = \boldsymbol{v}_j^{\Delta t} + 2\left(1 - \lambda_j\right)\left(\boldsymbol{n} \cdot \boldsymbol{v}_{\text{rel}}^{\Delta t}\right)\boldsymbol{n}$$
$$\boldsymbol{v}_{j+1}^{\text{col}} = \boldsymbol{v}_{j+1}^{\Delta t} + 2\lambda_j\left(\boldsymbol{n} \cdot \boldsymbol{v}_{\text{rel}}^{\Delta t}\right)\boldsymbol{n}$$

3h. Update positions for beads i, $i+1$, j, and $j+1$

$$\boldsymbol{x}^{\dagger} = \boldsymbol{x}^{\tau} + (\Delta t - \tau)\boldsymbol{v}^{\mathrm{col}}$$

3i. Calculate $\boldsymbol{v}^{\dagger}_{\mathrm{rel}}$, the relative velocity of the intersection point using velocities at the end of time step

$$\boldsymbol{v}^{\dagger}_{\mathrm{rel}} = \left(\boldsymbol{v}^{\dagger}_{j} - \boldsymbol{v}^{\dagger}_{i}\right) + \lambda_j\left(\boldsymbol{v}^{\dagger}_{j+1} - \boldsymbol{v}^{\dagger}_{j}\right) - \lambda_i\left(\boldsymbol{v}^{\dagger}_{i+1} - \boldsymbol{v}^{\dagger}_{i}\right)$$

3j. Update bead velocities at the end of the time step

$$\begin{aligned}
\boldsymbol{v}^{\ddagger}_{i} &= \boldsymbol{v}^{\dagger}_{i} + 2(1-\lambda_i)\left(\boldsymbol{n}\cdot\boldsymbol{v}^{\dagger}_{\mathrm{rel}}\right)\boldsymbol{n}\\
\boldsymbol{v}^{\ddagger}_{i+1} &= \boldsymbol{v}^{\dagger}_{i+1} + 2\lambda_i\left(\boldsymbol{n}\cdot\boldsymbol{v}^{\dagger}_{\mathrm{rel}}\right)\boldsymbol{n}\\
\boldsymbol{v}^{\ddagger}_{j} &= \boldsymbol{v}^{\dagger}_{j} - 2\left(1-\lambda_j\right)\left(\boldsymbol{n}\cdot\boldsymbol{v}^{\dagger}_{\mathrm{rel}}\right)\boldsymbol{n}\\
\boldsymbol{v}^{\ddagger}_{j+1} &= \boldsymbol{v}^{\dagger}_{j+1} - 2\lambda_j\left(\boldsymbol{n}\cdot\boldsymbol{v}^{\dagger}_{\mathrm{rel}}\right)\boldsymbol{n}
\end{aligned}$$

3k. If no collision occurs, then for beads i, $i+1$, j, and $j+1$

$$\begin{aligned}
\boldsymbol{v}^{\ddagger} &= \boldsymbol{v}^{\dagger}\\
\boldsymbol{x}^{\ddagger} &= \boldsymbol{x}^{\dagger}
\end{aligned}$$

4. Calculate the motion subject to the bead–surface uncrossability constraint to obtain $\boldsymbol{x}^{n+1}$ and $\boldsymbol{v}^{n+1}$.

RESULTS AND DISCUSSION

We have simulated a variety of fluid-polymer systems with this model. In simulations where complex fluid geometries occur, polymer-surface interactions are based on a level set representation of the domain boundary. The fluid dynamics simulation uses an embedded boundary formalism, with its own representation of the domain boundary. When sufficiently resolved, these representations are indistinguishable. Numerically, the differences converge at second order in grid spacing.

The hard constraint approach seems to be subject to a numerical stability problem which necessitates that the polymer dynamics set the time step, rather than the fluid dynamics. With a 100-bead polymer we find the polymer and fluid time steps to be comparable. But, with 200 beads the stable polymer time step is only 1/10 of the fluid-controlled value.

In order to demonstrate the hard constraint algorithm in 3D we present results for the particle algorithm alone, decoupled from the time-dependent fluid algorithm. Figure 1 is a time sequence of a bead–rod polymer in 3D with varying particle (bead) masses being transported by a uniform background flow. Initially the polymer is in a relaxed, stretched out state. The heavier particles at the head cause the non-trivial behavior as the polymer begins to tangle in time.

Figure 2 is a time sequence of single polymer transport in a 2D microscale flow with a cylindrical pillar obstruction that demonstrates intra-polymer and polymer–structure

Figure 1. Time sequence of a bead–rod polymer with varying particle masses in 3D. Polymer is initially stretched out but moves to a tangled state caused by transport of heavier particles up front in background flow.

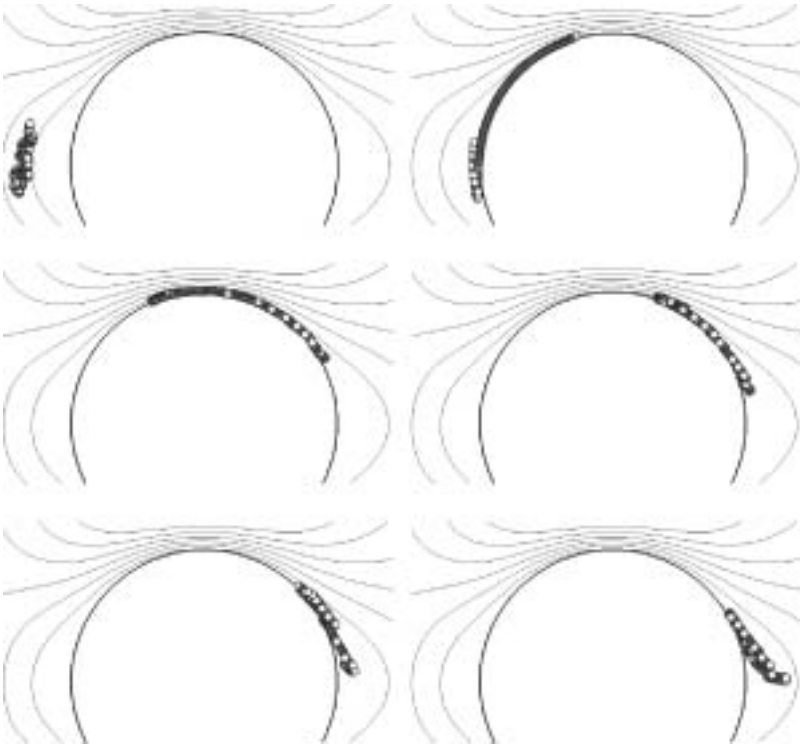

Figure 2. Time sequence of 200-bead polymer flowing past a cylinder in 2D with streamlines, demonstrating intra-polymer and polymer-structure interactions using smooth potential. From left to right, top to bottom: (a) Nearly entangled polymer. (b) Short-range polymer-surface interaction. (c) Acceleration around pillar due to Brownian perturbation and hydrodynamic drag. (d) More acceleration of the tail and slowing of the head in stagnation region in wake of pillar. (e) Accelerated tall catching up with stagnated head. (f) Re-entanglement in wake with multiple intra-polymer interactions.

interactions using the smooth potential hard constraint to prevent rod crossing. Time-dependent fluid coupling is included. In the first frame the polymer is randomly placed to be nearly entangled before flowing into the cylinder. Frame 2 shows a short-range

interaction of the polymer with the cylinder surface while also undergoing inter-polymer interactions. The polymer accelerates around the pillar in the third and fourth frames due to Brownian perturbation keeping it off the surface and nudging it out into the boundary layer where it is pulled by hydrodynamic drag. As the polymer approaches the near-stagnation wake region behind the pillar the head of the polymer begins to slow down allowing the tail to catch up in the fifth and then sixth frames. Re-entanglement occurs in the wake where numerous intra-polymer interactions occur.

CONCLUSION

We have demonstrated a new method based on a rigid constraint system to prevent rod-crossing in bead-rod polymer models in 3D. The rigid constraint algorithm is the simplest model that captures the essential properties of rod non-crossing. We use the same elastic collision model for rod non-crossing as in polymer-surface interactions. The model has a physical basis in early molecular dynamics simulations where hard spheres represent condensed matter. In this sense, hard constraints are a parameter-free end-member of parameter-dependent soft potentials.

The new hard constraint algorithm compares well, qualitatively, with expectations based on previous computations using soft potentials. It is difficult to see the differences during entanglement without establishing statistics from many simulations, which we did not perform here. Near surfaces, however, it is clear that the hard constraint allows the polymer to travel more closely to the surface where the fluid velocity is more nearly zero. At the resolution observable in these results, a smooth potential and the hard constraints described here give essentially identical results (differences are inevitable due to the stochastic terms in the fluid-particle coupling).

With the addition of these new force interactions, as expected, new highfrequency modes are introduced which limit stability and accuracy, necessitating adaptive time stepping strategies. Our numerical algorithm is computationally expensive: in each computational time step, an ${/mathcal O}(N^2)$ search is performed, iteratively. For systems containing a large number of interacting polymers, this computational bottle neck will present difficulties. While the hard constraint method eliminates those high-frequency modes which arise from soft potentials, we nevertheless find evidence of a time-step controlling instability. This may necessitate adaptive time stepping strategies. We have seen similar behavior as a side-effect of the Rouse bead-spring polymer model.

REFERENCES

1. D. Trebotich, G.H. Miller, P. Colella, D.T. Graves, D.F. Martin, and P.O. Schwartz, A Tightly Couple Particle-Fluid Model for DNA-Laden Flows in Complex Microscale Geometries, *Computational Fluid and Solid Mechanics*, pp. 1018–1022, 2005.
2. D. Trebotich, P. Colella, and G.H. Miller, A. Stable and Convergent Scheme for Viscoelastic Flow in Contraction Channels, *Journal of Computational Physics*, Vol. 205, pp. 315–342, 2005.
3. D. Trebotich and G.H. Miller, Modeling and Simulation of DNA Flow in a Microfluidic-Based Pathogen Detection System, *Proceedings of the 3rd Annual IEEE EMBS Special Topic Conference on Microtechnologies in Medicine and Biology*, pp. 353–355, 2005.

4. E.C. Lee and S.J. Muller, Flow Light Scattering Studies of Polymer Coil Conformation in Solutions in Extensional Flow, *Macromolecules*, Vol. 32, pp. 3295–3305, 1999.
5. M. Somasi, B. Khomami, N.J. Woo, J.S. Hur, and E.S.G. Shaqfeh, Brownian Dynamics Simulations of Bead-Rod and Bead-Spring Chains: Numerical Algorithms and Coarse-Graining Issues, *Journal of Non-Newtonian Fluid Mechanics*, Vol. 108, pp. 227–255, 2002.
6. M. Mazars, Freely Jointed Chains in External Potentials: Analytical Computations, *Journal of Physics A: Mathematical and General*, Vol. 32, pp. 1841–1861, 1999.
7. M.D. Bybee, G.H. Miller, and D. Trebotich, Particle Interactions in DNA Flows, Technical Report UCRL-TR-217843, Lawrence Livermore National Laboratory, Livermore, California, USA, December 2005.
8. S. Kumar and R. G. Larson, Brownian Dynamics Simulations of Flexible Polymers with Spring-Spring Repulsions, *Journal of Chemical Physics*, Vol. 114(15), pp. 6937–6941, 2001.
9. J.T. Padding and W.J. Briels, Uncrossability Constraints in Mesoscopic Polymer Melt Simulations: Non-Rouse Behavior of C_{120} H_{242}, *Journal of Chemical Physics*, Vol. 115(6), pp. 2846–2859, 2001.